arXiv:1703.04989v1 [hep-ph] 15 Mar 2017

March 14, 2017

Analysis of $\gamma\gamma \to ZH$ within the CSM concept.

F.M. Renard

Laboratoire Univers et Particules de Montpellier, UMR 5299
Université Montpellier II, Place Eugène Bataillon CC072
F-34095 Montpellier Cedex 5, France.

Abstract

We study the modifications of the $\gamma\gamma \to ZH$ amplitudes and cross sections generated by Higgs and top quark compositeness in particular within the CSM concept. We insist on the particular interest of polarized photon-photon collisions which should allow to identify the origin of the large observable differences between various, CSM conserving or CSM violating, compositeness possibilities.

PACS numbers: 12.15.-y, 12.60.-i, 14.80.-j; Composite models

1 INTRODUCTION

In previous papers we have studied the effect of Higgs boson and top quark compositeness on ZH production in gluon-gluon collision, [1], [2]. We have introduced the concept of Composite Standard Model (CSM) which should preserve the structure and the main properties of the Standard Model (SM), at least at low energy. No anomalous coupling modifying the SM structures should be present, but form factors (for example due to substructures) would affect the Higgs boson and top quark couplings at high energy. We had not based our analyzes on a specific compositeness model, for example one of those mentioned in ref. [3, 4, 5, 6, 7, 8], but on the dependence of the observables on form factor effects.

We had noticed that the $gg \to ZH$ process is particularly sensitive to the presence of form factors, because they could destroy a peculiar SM cancellation between diagrams involving Higgs boson and top quark couplings. But we had also shown that this cancellation can be recovered provided that a special relation between form factors is satisfied. We considered this relation as a specific CSM property.
This $gg \to ZH$ process is therefore very interesting for revealing a violation of the SM prediction but an amplitude analysis confirming the origin of such an effect seems difficult to do in hadronic collisions.

This is why, in the present paper, we make an analysis of $\gamma\gamma \to ZH$, the similar process appearing in photon-photon collisions.
The possibility of high energy photon-photon collisions has been considered since a long time, [9]; for a recent review see [10].
Its very interesting feature for our purpose is the possibility of working with polarized beams; this would allow to make an amplitude analysis and to check what happens with the above mentioned cancellation.
This will be essential for choosing among the various compositeness possibilities, for example either with only t_R or with both t_L and t_R compositeness, and with or without the CSM constraint relating it to Higgs compositeness.

Contents: In Section 2 we recall the definitions and the SM properties of the amplitudes and observables of the $\gamma\gamma \to ZH$ process with polarized beams. In Section 3 we define the form factors, with or without the CSM constraint, that would affect the amplitudes. Illustrations showing their effect on the observables are given in Section 4, and the conclusion and outlook in Section 5.

2 AMPLITUDES AND OBSERVABLES OF THE $\gamma\gamma \to ZH$ PROCESS

At one loop order the SM amplitudes of the $\gamma\gamma \to ZH$ process arise from the charged fermion (leptons and quarks) loop diagrams depicted in Fig.1; triangle diagrams (a),(b) and box diagrams (c), (with gluon-gluon symmetrization); see [11] and older references therein.

With CP conservation and Bose statistics the helicity amplitudes $F_{\lambda,\lambda',\tau}$ for γ,γ,Z helicities $\lambda,\lambda' = \pm\frac{1}{2}$ and $\tau = 0,\pm 1$ satisfy the following relations

$$F_{---} = F_{+++} \quad F_{--0} = -F_{++0} \quad F_{--+} = F_{++-} \tag{1}$$

$$F_{-+-} = F_{+-+} \quad F_{-+0} = -F_{+-0} \quad F_{-++} = F_{+--} \tag{2}$$

$$F_{\lambda,\lambda',\tau}(\theta) = (-1)^{\tau} F_{\lambda',\lambda,\tau}(\pi - \theta) \tag{3}$$

The polarized cross section has the following structure

$$\begin{aligned}
\frac{d\sigma(\gamma\gamma \to ZH)}{d\cos\theta} &= \frac{d\sigma_0}{d\cos\theta} + \langle \xi_2 \xi_2' \rangle \frac{d\sigma_{22}}{d\cos\theta} \\
&\quad - \langle \xi_3 \rangle \frac{d\sigma_3}{d\cos\theta} \cos 2\phi - \langle \xi_3' \rangle \frac{d\sigma_3'}{d\cos\theta} \cos 2\phi' \\
&\quad + \langle \xi_3 \xi_3' \rangle \Big[\frac{d\sigma_{33}}{d\cos\theta} \cos(2[\phi + \phi']) + \frac{d\sigma_{33}'}{d\cos\theta^*} \cos(2[\phi - \phi']) \Big] \\
&\quad + \langle \xi_2 \xi_3' \rangle \frac{d\sigma_{23}}{d\cos\theta} \sin 2\phi - \langle \xi_3 \xi_2' \rangle \frac{d\sigma'_{23}}{d\cos\theta} \sin 2\phi' \quad .
\end{aligned} \tag{4}$$

where (ξ_2, ξ_2'), $(\xi_3,\ \xi_3')$ and $(\phi,\ \phi')$ describe respectively the average helicities, transverse polarizations and azimuthal angles of the two photons with their density matrices

$$\rho = \frac{1}{2} \begin{pmatrix} 1+\xi_2 & -\xi_3 e^{-2i\phi} \\ -\xi_3 e^{2i\phi} & 1-\xi_2 \end{pmatrix} \qquad \rho' = \frac{1}{2} \begin{pmatrix} 1+\xi_2' & -\xi_3' e^{2i\phi'} \\ -\xi_3' e^{-2i\phi'} & 1-\xi_2' \end{pmatrix} \tag{5}$$

Using the above CP conservation relations the σ_n-quantities in (4) are defined as

$$\frac{d\sigma_0}{d\cos\theta} = \left(\frac{\beta}{64\pi s}\right) \sum_{\tau} [\ |F_{++\tau}|^2 + |F_{+-\tau}|^2\ ] \tag{6}$$

$$\frac{d\sigma_{22}}{d\cos\theta} = \left(\frac{\beta}{64\pi s}\right) \sum_{\tau} [\ |F_{++\tau}|^2 - |F_{+-\tau}|^2\ ] \tag{7}$$

$$\frac{d\sigma_3}{d\cos\theta} = \left(\frac{\beta}{32\pi s}\right) \sum_{\tau} Re[F_{++\tau} F^*_{-+\tau}] \tag{8}$$

$$\frac{d\sigma'_3}{d\cos\theta} = \left(\frac{\beta}{32\pi s}\right)\sum_\tau Re[F_{++\tau}F^*_{+-\tau}] \tag{9}$$

$$\frac{d\sigma_{33}}{d\cos\theta} = \left(\frac{\beta}{64\pi s}\right)\sum_\tau Re[F_{+-\tau}F^*_{-+\tau}\,] \tag{10}$$

$$\frac{d\sigma'_{33}}{d\cos\theta} = \left(\frac{\beta}{64\pi s}\right)\sum_\tau Re[F_{++\tau}F^*_{--\tau}\,] \tag{11}$$

$$\frac{d\sigma_{23}}{d\cos\theta} = \left(\frac{\beta}{32\pi s}\right)\sum_\tau Im[F_{++\tau}F^*_{+-\tau}] \tag{12}$$

$$\frac{d\sigma'_{23}}{d\cos\theta} = \left(\frac{\beta}{32\pi s}\right)\sum_\tau Im[F_{++\tau}F^*_{-+\tau}] \tag{13}$$

with

$$\beta = \sqrt{\left[1-\frac{(m_Z-m_H)^2}{s}\right]\left[1-\frac{(m_Z+m_H)^2}{s}\right]} \quad , \tag{14}$$

Note that $d\sigma_0/d\cos\theta$, $d\sigma_{22}/d\cos\theta$, $d\sigma_{33}/d\cos\theta$ and $d\sigma'_{33}/d\cos\theta$ are symmetric under the interchange

$$\theta \leftrightarrow \pi - \theta \quad ,$$

whereas

$$\frac{d\sigma_3}{d\cos\theta}\Big|_\theta = \frac{d\sigma'_3}{d\cos\theta}\Big|_{\pi-\theta} \quad ,$$
$$\frac{d\sigma_{23}}{d\cos\theta}\Big|_\theta = \frac{d\sigma'_{23}}{d\cos\theta}\Big|_{\pi-\theta} \quad .$$

As in the $gg \to ZH$ case the leading contributions come from top quark loops in (a) and (c) whereas the (b) contribution is much smaller. This smallness arises from the mass suppressed ZZH coupling appearing in (b) as compared to the G^0ZH one in (a) which has in addition the (m_t/m_W) enhancement due to the G^0tt coupling.

The triangle diagrams (a) and (b) only contribute to the $F_{\pm\pm0}$ amplitudes whereas the boxes (c) contribute to all amplitudes.

The real and imaginary parts of the resulting SM amplitudes are shown in Fig.2a,b. One can see that the helicity concerving (HC) amplitudes $F_{\pm\mp0}$ finally dominate over the helicity violating (HV) ones at high energy in agreement with the HC rule [12].

The remarkable cancellation between contributions of diagrams (a) and (c) is illustrated in Fig.3a,b.

The energy and angular dependences of the various σ_n elements of the polarized cross section are shown in Fig.4-5. As in the $gg \to ZH$ case the rate of longitudinal Z production is always very large, apart from local energy and angular fluctuations. We only illustrate its shapes for σ_0 when looking at the form factor effects in Fig.8a,b.

All these behaviours are globally similar to those of the $gg \to ZH$ process. Only small differences appear at low energy where the effect of light lepton and quark loops is not totally negligible.

3 CSM CONSTRAINTS

Let us first recall the procedure used in [2] for introducing this CSM concept in the previous analysis of the $gg \to ZH$ process.

We affect form factors to each coupling appearing in the one loop diagrams of this process (see Fig.1) and involving an Higgs boson and/or a top quark. This means five arbitrary form factors chosen as $F_{G^0Z_LH}(s) = F_{ZZ_LH}(s), F_{Htt}(s), F_{Gtt}(s), F_{tR}(s), F_{tL}(s)$.

Incidently we note that photon-tt form factors (similarly to gluon-tt form factors) may also appear, but as they would occur exactly in the same way in the triangles and in the boxes, they would not affect the structures of the amplitudes (in particular the special cancellation mentioned in the previous section); they would only modify the total result by a pure normalization factor. So we do not discuss them more.

With the five arbitrary form factors listed above large effects are in general observed due to the destruction of the cancellation appearing for the F_{++0} amplitude between its contribution from triangle (a) and the one from boxes (c) (see Fig.8 of [2]). But this cancellation can be recovered provided that the following CSM constraint is satisfied:

$$F_{G^0Z_LH}(s)F_{Gtt}(s)(g^Z_{tR} - g^Z_{tL}) = F_{Htt}(s)(g^Z_{tR}F_{tR}(s) - g^Z_{tL}F_{tL}(s)) \tag{15}$$

We now look at the $\gamma\gamma \to ZH$ process and the effect of such form factors, with and without the CSM constraint, on the observables defined in the previous section.

For the illustrations, as simple examples, we will use simple "test" expressions of the type

$$F(s) = \frac{(m_Z + m_H)^2 + M^2}{s + M^2} \tag{16}$$

with the new physics scale M taken for example with the value of 5 TeV.
We use this expression for different form factors and we treat separately the following

cases:

The two CSM conserving cases will be

— (a) denoted CSMtLR, refering to both t_L and t_R compositeness, with $F_{tR}(s) = F_{tL}(s) \equiv F(s)$, and $F_{G^0Z_LH}(s) = F_{Gtt}(s) = F_{Htt}(s) \equiv F(s)$ satisfying (15),

— (b) denoted CSMtR, for pure t_R compositeness, $F_{tR}(s) \equiv F(s)$ and $F_{tL}(s) = 1$, and, in order to satisfy (15), either
$F_{Gtt}(s) = F_{Htt}(s) \equiv F(s)$ and $F_{G^0Z_LH}(s)(g^Z_{tR} - g^Z_{tL}) = g^Z_{tR}F_{tR}(s) - g^Z_{tL}$
or
$F_{G^0Z_LH}(s) = F_{Htt}(s) \equiv F(s)$ and $F_{Gtt}(s)(g^Z_{tR} - g^Z_{tL}) = g^Z_{tR}F_{tR}(s) - g^Z_{tL}$,

and the 2 CSM violating cases:

— (c) denoted CSMvt, where $F_{tR}(s)$ with $M = 10$ TeV, $F_{tL}(s)$ with $M = 15$ TeV and $F_{G^0Z_LH}(s) = F_{Htt}(s) = F_{Gtt}(s) \equiv F(s)$ with $M = 5$ TeV,

— (d) denoted CSMvH, no top form factor and only one $F(s)$ form factor affecting the G^0Z_LH and ZZ_LH vertices.

In the next Section and Figures 6-8, we illustrate the consequences of such choices for the observables.

4 ILLUSTRATIONS

Fig.6a-f and 7a-f respectively illustrate the effects of the choices (a-d) of form factors on the energy and angular dependences of the σ_n cross sections corresponding to the unpolarized or to specific polarization cases. Fig.8a,b illustrate similarly the behaviour of the Z_L rate in the σ_0 cross section.

As in the gluon-gluon case we can first check that the unpolarized σ_0 cross section is very sensitive to the CSM violation cases CSMvt and CSMvH. The corresponding Z_L rates tend also to be closer to 1 at high energy.
Similar effects can be seen in the longitudinal polarization term σ_{22}.
The transverse polarization terms σ_3 (related to σ'_3) and σ'_{33} are also very sensitive with spectacular changes of signs.
On the opposite the double transverse σ_{33} term, only controlled by HC amplitudes, is not affected by the CSMvH case, but gets some effects in the other cases.
The mixed longitudinal and transverse term σ_{23} (related to σ'_{23}) involving both HV and HC amplitudes get also notably modified by the CSM violating terms.

Globally the CSM conserving terms lead to weaker effects in these various cross section elements.

Quantitatively the above effects obviously depend on the precise expression used for the "test" form factor and on the value of M; our simple choice has no physical meaning but was only chosen in order to show the sensitivity of each observable.

Note also that the CSM violating cases producing large differences with the pure SM prediction due to the destruction of the special cancellation in $F_{\pm\pm 0}$ amplitudes could nevertheless satisfy unitarity owing to the decrease of the form factors above the new physics scale (chosen at 5 TeV in the illustrations).

5 CONCLUSIONS

We have shown that the $\gamma\gamma \to ZH$ process, especially with polarized photon beams, should be particularly interesting for analyzing a possible departure from SM predictions with the aim of testing the CSM concept.
Indeed the observables of the $\gamma\gamma \to ZH$ process with photon polarizations and the associated θ, ϕ, ϕ' dependences should allow to make an amplitude analysis and to identify the form factor structure, CSM conserving or CSM violating.
As in the $gg \to ZH$ case, the biggest effect should be found in the $F_{\pm\pm 0}$ amplitude whose internal cancellation property is preserved or violated by the corresponding form factors.
We have illustrated with a simple "test" shape how the various observables react to the presence of a form factor in the involved couplings.
We can conclude, in the case a departure from SM prediction would be observed in $gg \to ZH$, that the $\gamma\gamma \to ZH$ process would be very fruitful for revealing the nature of a possible compositeness interpretation.

Along this line of thought further works could be carried with phenomenological analyzes of other processes sensitive to such compositeness effects, with or without CSM constraint; see for example $WW, ZZ \to t\bar{t}$ and ref.[14]. Independently, possible theoretical studies could be done about the meaning of the CSM concept.

References

[1] F.M. Renard, arXiv: 1701.04571.

[2] F.M. Renard, arXiv: 1701.09116, 1702.08853.

[3] G. Panico and A. Wulzer, Lect.Notes Phys. **913**,1(2016).

[4] H. Terazawa, Y. Chikashige and K. Akama, Phys. Rev. **D15**, 480 (1977); for other references see H. Terazawa and M. Yasue, Nonlin.Phenom.Complex Syst. **19**,1(2016); J. Mod. Phys. **5**, 205 (2014).

[5] D.B. Kaplan and H. Georgi, Phys. Lett. **136B**, 183 (1984).

[6] K. Agashe, R. Contino and A. Pomarol, Nucl. Phys. **B719**, 165 (2005); hep/ph 0412089.

[7] R. Contino, T. Kramer, M. Son and R. Sundrum, J. High Energy Physics **05**(2007)074.

[8] G. Panico and A. Wulzer, Lect.Notes Phys. **913**,1(2016).

[9] I.F. Ginzburg, G.L. Kotkin, V.G. Serbo and V.I. Telnov, Nucl. Instr. and Meth. **205**, 47 (1983); I.F. Ginzburg, G.L. Kotkin, V.G. Serbo, S.L. Panfil and V.I. Telnov, Nucl. Instr. and Meth. **219**,5 (1984); J.H. Kühn, E.Mirkes and J. Steegborn, Z. f. Phys. **C57**, 615 (1993).

[10] V.I. Telnov, Nucl.Part.Phys.Proc. **273**(2016)219.

[11] G.J. Gounaris, P.I. Porfyriadis and F.M. Renard, Eur. Phys. J. **C20**, 659 (2001),

[12] G.J. Gounaris and F.M. Renard, Phys. Rev. Lett. **94**, 131601 (2005), hep-ph/0501046; Phys. Rev. **D73**, 097301 (2006) , hep-ph/0604041.

[13] M. Hoffmann, A. Kaminska, R. Nicolaidou and S. Paganis, Eur. Phys. J. **C74**, 3181 (2014); arXiv: 1407.8000.

[14] G.J. Gounaris and F.M. Renard, Phys. Rev. **D94**, 053009 (2016).

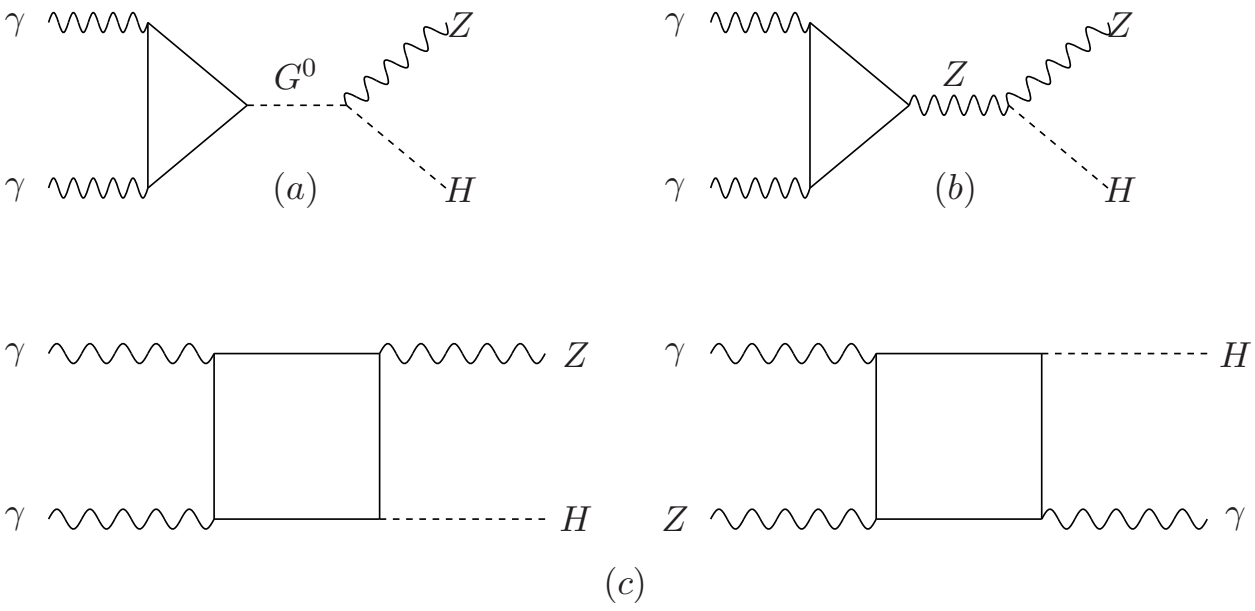

Figure 1: The triangle and box one loop SM diagrams contributing to the $\gamma\gamma \to ZH$ process.

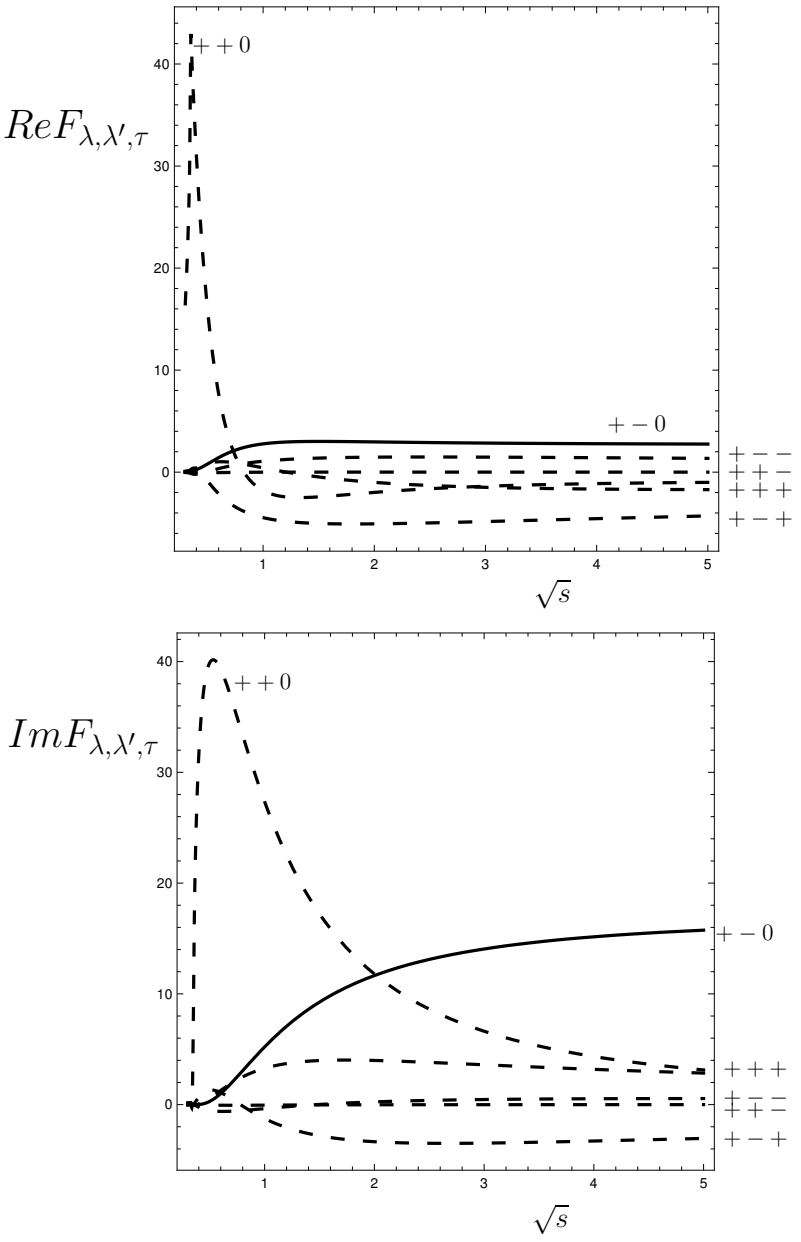

Figure 2: Energy dependence of the real and imaginary parts of the 6 independent SM amplitudes.

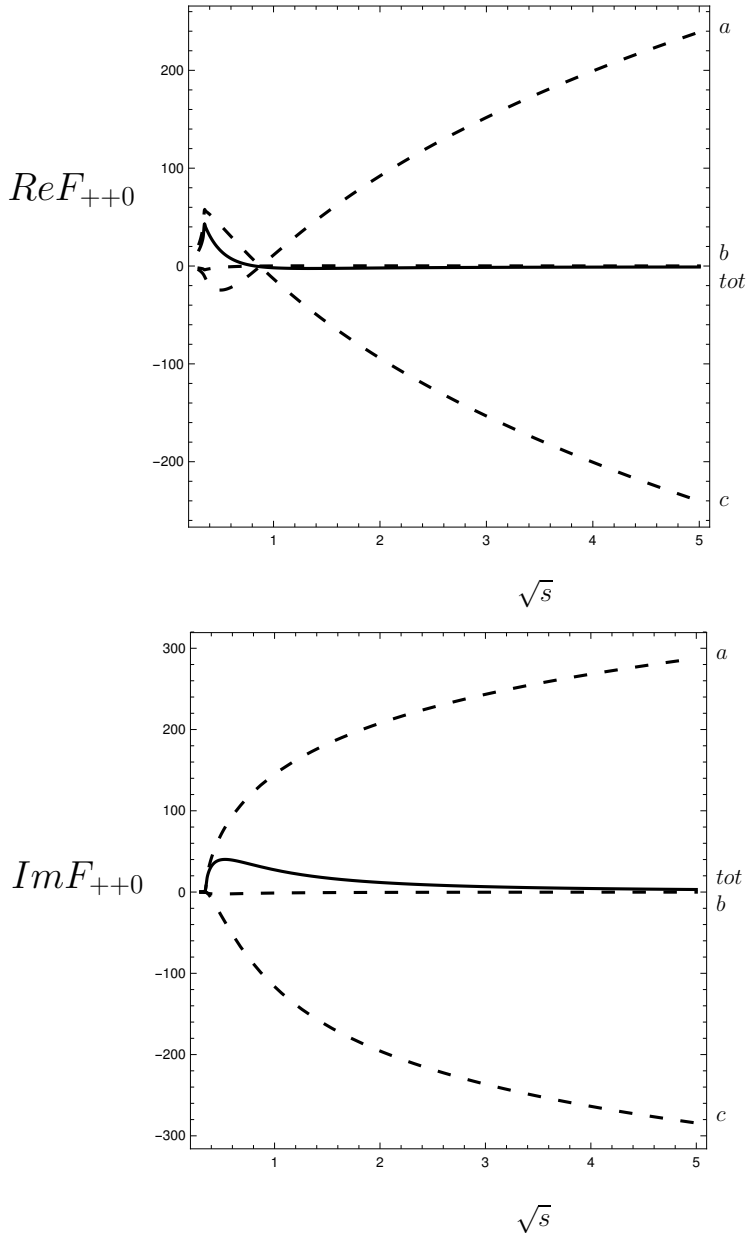

Figure 3: Energy dependences of the real and imaginary parts of the SM contributions to the F_{++0} amplitude; (a),(b),(c) diagrams and total.

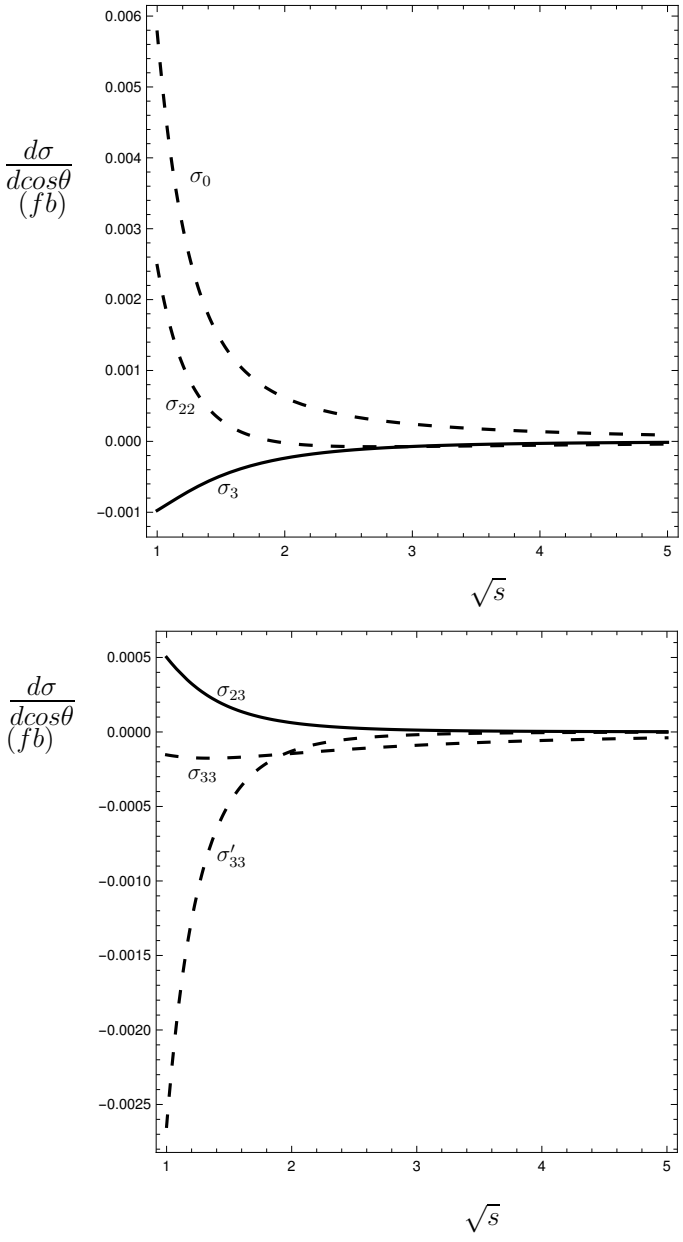

Figure 4: Energy dependence of SM cross sections.

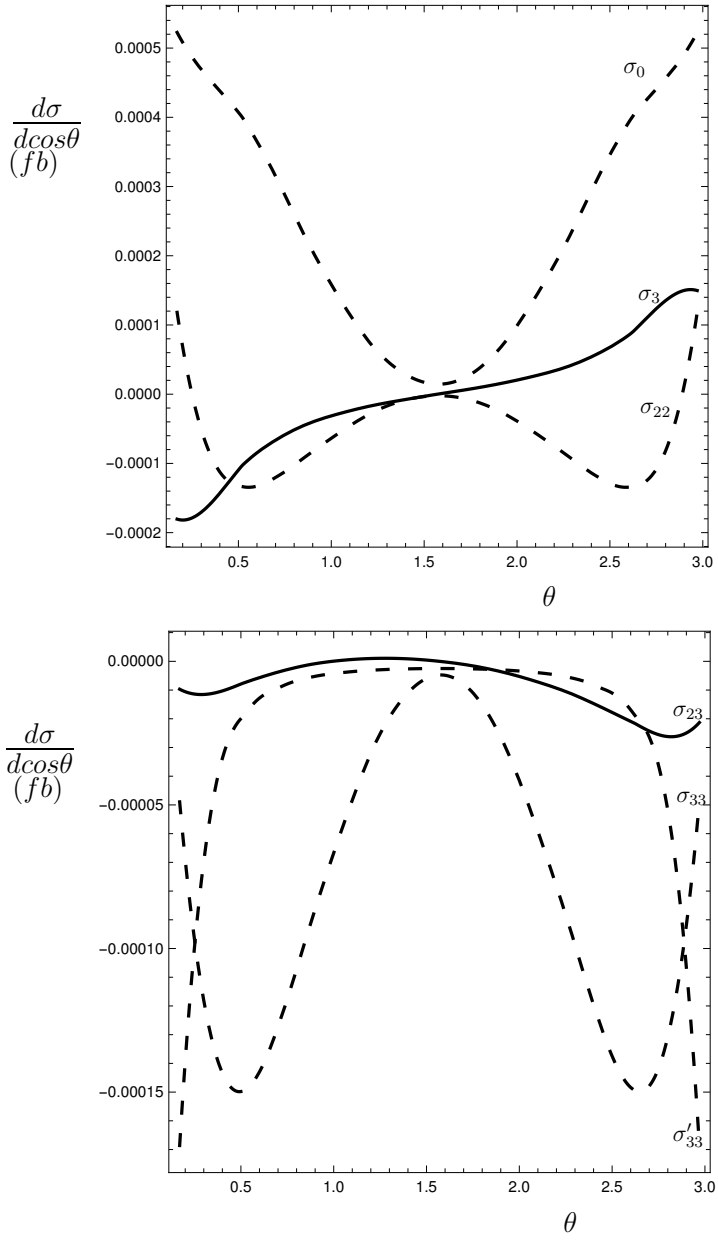

Figure 5: Angular distributions of SM cross sections at 4 TeV.

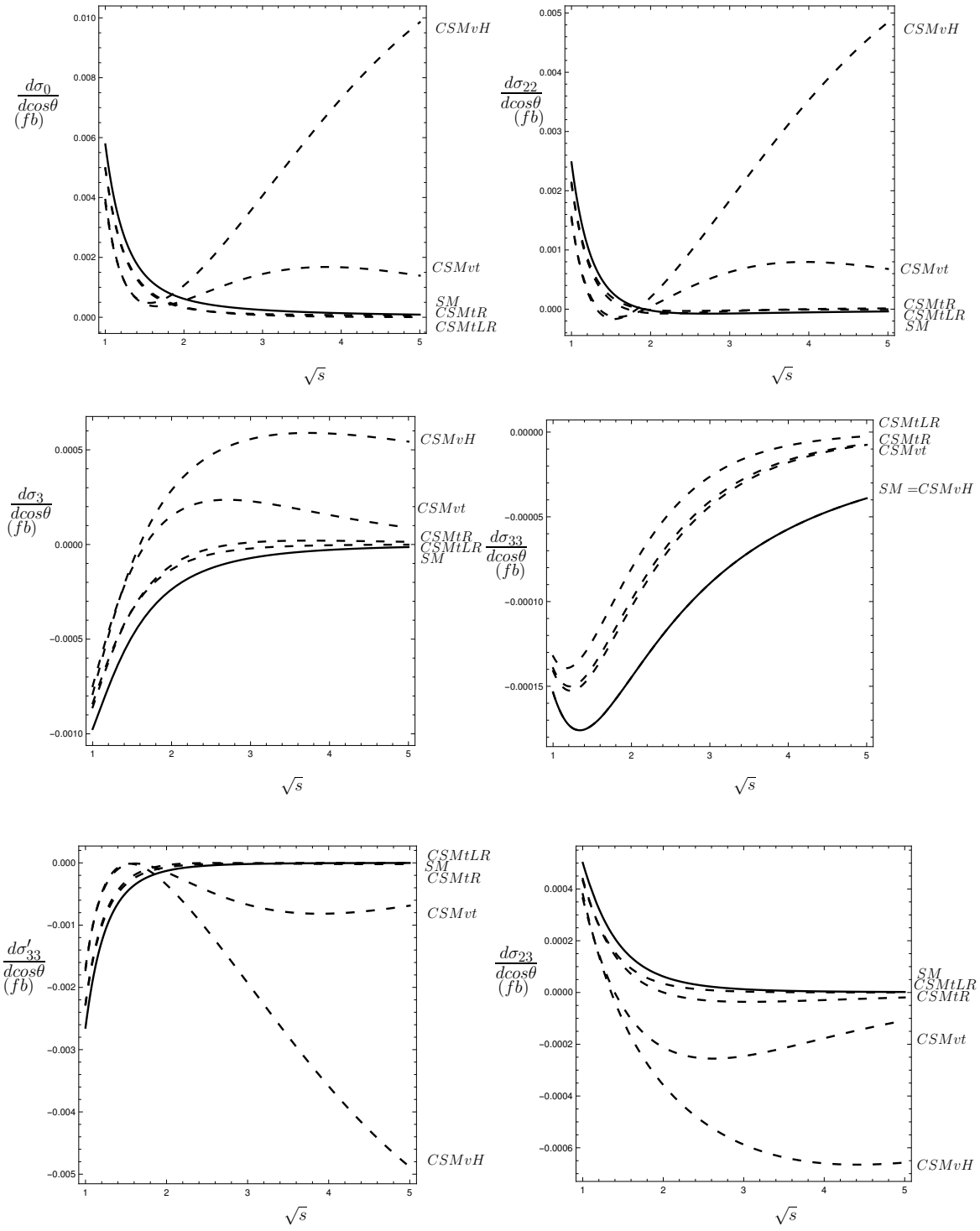

Figure 6: Cross sections in SM, CSMtLR, CSMtR, CSMvt, CSMvH cases.

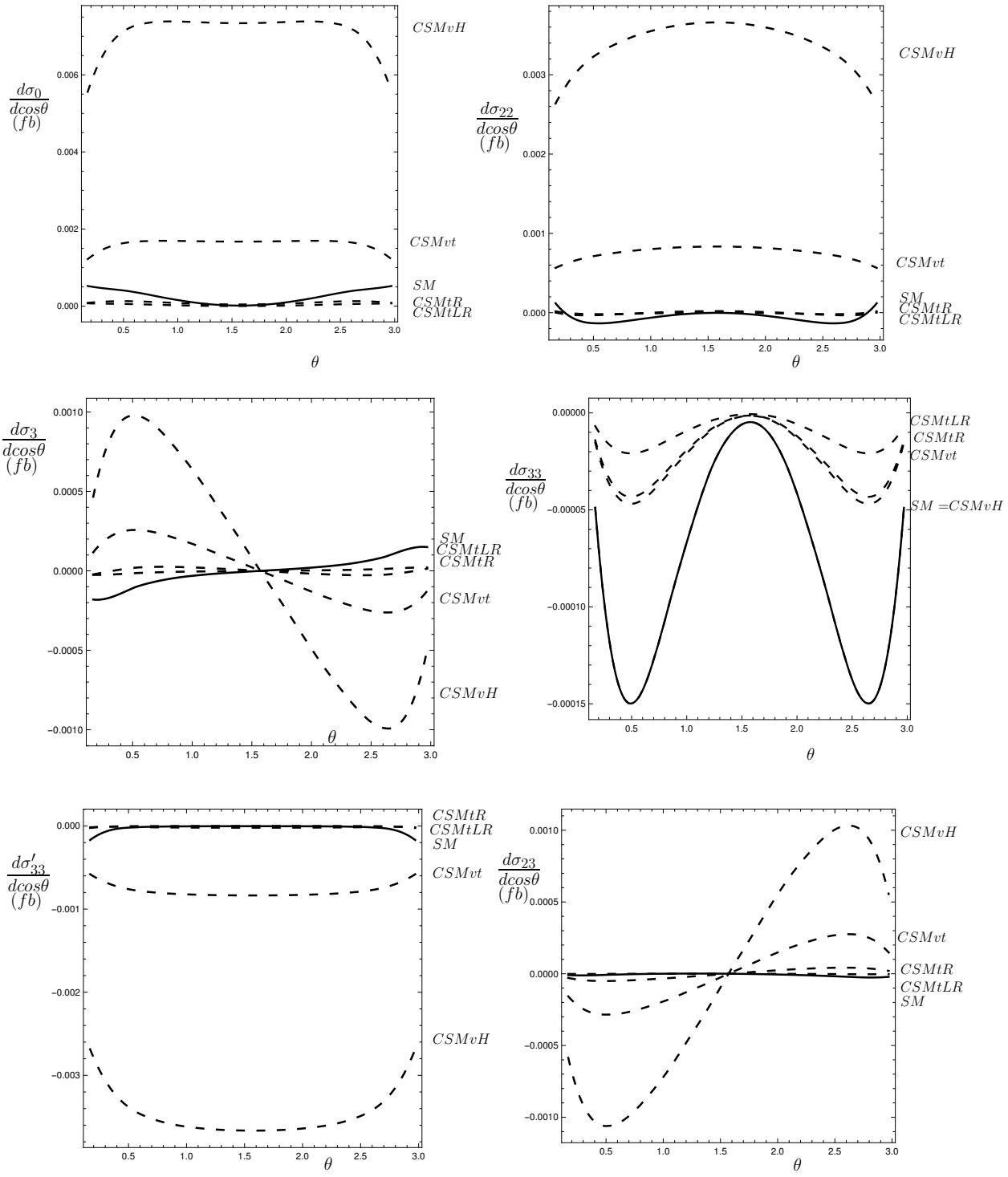

Figure 7: Angular distributions in SM, CSMtLR, CSMtR, CSMvt, CSMvH cases.

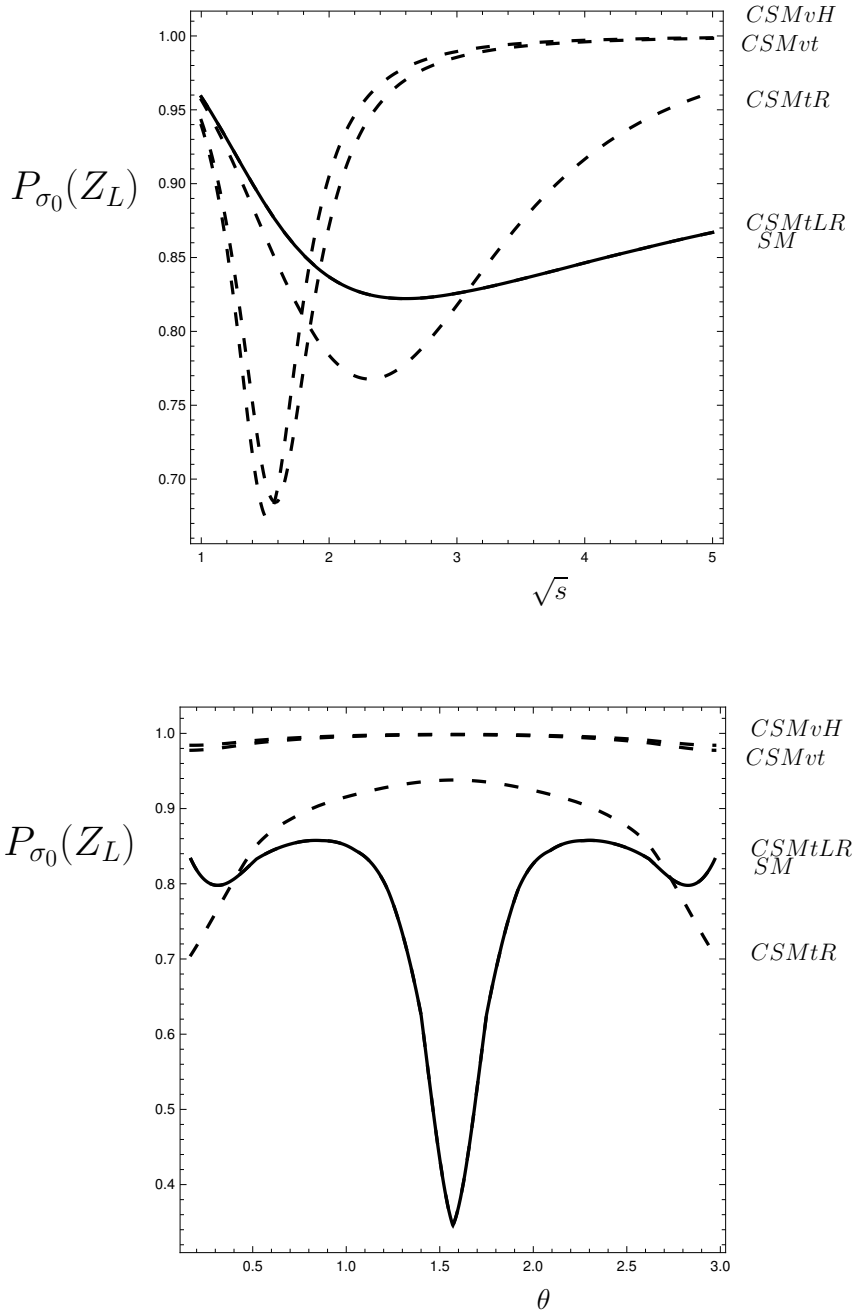

Figure 8: Energy dependence and angular distribution of Z_L rate of σ_0 in SM, CSMtLR, CSMtR, CSMvt, CSMvH cases.